

Design of Orthogonal Pulse Shapes for Communications via Semidefinite Programming

Timothy N. Davidson, *Member, IEEE*, Zhi-Quan (Tom) Luo, *Member, IEEE*, and
Kon Max Wong, *Senior Member, IEEE*

Abstract—In digital communications, orthogonal pulse shapes are often used to represent message symbols for transmission through a channel. In this paper, the design of such pulse shapes is formulated as a convex semidefinite programming problem, from which a globally optimal pulse shape can be efficiently found. The formulation is used to design filters that achieve

- a) the minimal bandwidth for a given filter length;
- b) the minimal filter length for a given bandwidth;
- c) the maximal robustness to timing error for a given bandwidth and filter length.

Bandwidth is measured either in spectral energy concentration terms or with respect to a spectral mask. The effectiveness of the method is demonstrated by the design of waveforms with substantially improved performance over the “chip” waveforms specified in recent standards for digital mobile telecommunications.

Index Terms—Code division multiaccess, multirate FIR digital filters, optimization methods, pulse amplitude modulation, signal design.

I. INTRODUCTION

ONE OF THE fundamental operations in digital communications is the representation of a message symbol by an analog waveform for transmission through a channel (waveform coding) [1], [2]. The choice of such waveforms critically affects the performance of a communications scheme and usually involves a compromise between system capacity, robustness to expected channel imperfections and interference, system delay, and transmitter and receiver complexity. The most common waveform coding techniques involve linear pulse amplitude modulation of a self-orthogonal (“root Nyquist”) waveform or an approximation thereof. In conventional communication systems, the available analog waveform coding technology has tended to restrict orthogonal waveform design to a choice among a small set of waveforms. However, the increasing deployment of baseband digital signal processors has extended the class of waveforms that can be easily implemented. In such a situation, the design of the waveform can be transformed to the design of an orthogonal multirate discrete-time finite impulse response (FIR) filter [3], [4]. Unlike conventional single-rate FIR filter design objectives, which can often be formulated as optimization problems with analytic or computationally

efficient solutions [5]–[7], the orthogonal multirate FIR filter design problem has a translation orthogonality constraint [3], [4], which is not convex. Such nonconvexity can lead to the standard problems of local minima in the design process.

Fortunately, many of the desirable properties of an orthogonal waveform are actually properties of the autocorrelation of the waveform. By reformulating the design problem in terms of the autocorrelation sequence of the “pulse-shaping” filter, the translation orthogonality constraints become linear and, hence, convex. Once the autocorrelation sequence has been designed, the transmission and reception filters can be extracted (nonuniquely) by spectral factorization. In this way, many pulse-shaping filter design problems can be formulated as linearly constrained convex minimization problems [8]–[13]. Unfortunately, an infinite set of linear constraints is required to ensure that the designed autocorrelation has a spectral factor, and such sets can be rather awkward to deal with in practice [8], [14]. In this paper, we employ a state space parameterization of the autocorrelation sequence and use the positive-real lemma [15] to transform the semi-infinite linear constraint into a finite linear matrix inequality. The transformed (autocorrelation design) problem is a convex semidefinite program (SDP) [16] whose globally optimal solution can be found in an efficient manner using interior point methods [17]. Furthermore, the minimum-phase spectral factor can be extracted directly from the output of the optimization routine by using a result of Anderson *et al.* [18]. This renders the auxiliary spectral factorization step unnecessary. We point out that the positive-real lemma has been briefly proposed for the transformation of conventional single-rate FIR filter design problems from semi-infinite convex programs [19] to SDP’s [20] without the direct extraction of the minimum-phase spectral factor. We also point out that the autocorrelation sequences that we design fall into a subclass of linear-phase Nyquist filters. The design of a general Nyquist filter does not require the “spectral factorizability” constraint and, therefore, tends to be simpler [21]–[27] (especially in the linear phase case), but the resulting transmission and reception filters may have different spectra.

We will show that many important pulse-shaping filter design problems can be cast as a sequence of semidefinite feasibility problems and, hence, can be solved efficiently. The problems considered here include finding filters that achieve

- a) the minimal bandwidth for a given filter length;
- b) the minimum filter length required to achieve a certain bandwidth;
- c) the maximal robustness to timing error for a given filter length and bandwidth.

Manuscript received March 18, 1999; revised October 14, 1999. This work was supported by a research grant from Natural Sciences and Engineering Research Council of Canada and a grant from Telecommunications Research Institute of Ontario (TRIO). The associate editor coordinating the review of this paper and approving it for publication was Dr. Alle-Jan van der Veen.

The authors are with the Department of Electrical and Computer Engineering, McMaster University, Hamilton, Ont., Canada L8S 4L7.

Publisher Item Identifier S 1053-587X(00)03326-2.

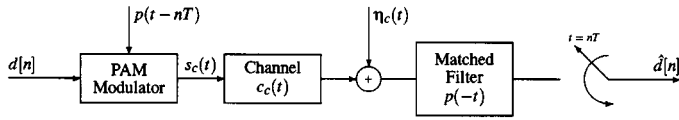


Fig. 1. Model of a baseband digital communication scheme.

Here, bandwidth is measured either in spectral energy concentration terms or with respect to a spectral mask. We also show that simple modifications to the design framework allow compensation for nonideal characteristics of the analog smoothing filter at the transmitter and antialiasing filter at the receiver. The applicability of our techniques are demonstrated in several examples in which we design “chip” waveforms with superior performance to those specified in recent standards for code division multiple access (CDMA)-based mobile telephony [28], [29].

In related work, the problem of maximizing the percentage of signal energy in a given bandwidth, subject to the orthogonality constraints, has previously been posed as a nonconvex constrained optimization problem [3], [4]. In this paper, however, we show that it can also be formulated as a convex SDP and, hence, efficiently solved. An alternative semi-infinite linear programming (SILP) formulation can be extracted from [13]. (The design of a more general Nyquist filter with this objective results in an eigenvalue problem [21], [23], [25].) When the energy bandwidth criterion is replaced by certain spectral mask measures of bandwidth, pulse-shaping filters can be found via SILP [8] via modified Remez algorithms [9], [12] or via an SDP (see Problem 4 in Section IV-B), with the finite nature of the “spectral factorizability” constraint being an advantage of the SDP.

II. BASEBAND PULSE AMPLITUDE MODULATION

Consider the standard model for a baseband digital communication scheme in Fig. 1. For notational convenience, we consider only real-valued systems, but the methods can be extended to the complex-valued case in a straightforward manner. We allow (finitely) noncausal filters in our model with the understanding that an appropriate delay will be required for implementation. The data are waveform coded by pulse amplitude modulation (PAM) as

$$s_c(t) = \sum_n d[n]p(t - nT) \quad (1)$$

and are transmitted through a linear time-invariant (LTI) baseband equivalent channel $c_c(t)$ with additive noise and interference modeled by $\eta_c(t)$. The received signal is passed through the “matched” filter $p(-t)$ and is synchronously sampled to form the data estimate $\hat{d}[n]$. Such a scheme can be conveniently implemented using digital signal processors (DSP’s) at the transmitter and receiver, as shown in Fig. 2, where the filter $g[k]$ has a finite impulse response (FIR) of length L

$$p(t) = \sum_{k=0}^{L-1} g[k]\phi_s(t - kT/N) \quad (2)$$

and the matched filter is $\sum_k g[-k]\phi_r(kT/N - t) \approx p(-t)$.

Here

$\phi_s(t)$ smoothing filter in the digital-to-analog converter (DAC);

N oversampling rate;

$\phi_r(-t)$ “anti-aliasing” filter at the receiver.

For that implementation, we can form an equivalent discrete-time model in which $s[k] = \sum_n d[n]g[k - Nn]$ is deemed to be the transmitted signal, and $c[k] = (\phi_r(-t) \star c_c(t) \star \phi_s(t))|_{t=kT/N}$, where \star denotes convolution, is the discrete-time equivalent channel, which can be written as

$$c[k] = \int c_c(\tau)r_{\phi_s\phi_r}(\tau - kT/N) d\tau \quad (3)$$

where $r_{\phi_s\phi_r}(\tau) \triangleq \int \phi_s(\lambda)\phi_r(\lambda + \tau) d\lambda$. The received version of $s[k]$ is $\hat{s}[k] = \sum_m c[k - m]s[m] + \eta[k]$, where $\eta[k] = \int \eta_c(t)\phi_r(t - kT/N) dt$. The data estimates are then given by $\hat{d}[n] = \sum_k g[k - Nn]\hat{s}[k]$, which can be written as

$$\hat{d}[n] = \sum_q c_{\text{ISI}}[n - q]d[q] + \eta_d[n] \quad (4)$$

where $c_{\text{ISI}}[q] = \sum_i c[i]r_g[i - Nq]$ is the equivalent channel from an inter-symbol interference (ISI) perspective, $r_g[m] \triangleq \sum_k g[k]g[k + m]$ is the autocorrelation sequence of the filter $g[k]$, and $\eta_d[n] = \sum_k g[k - Nn]\eta[k]$ is the effect of the noise on $\hat{d}[n]$.

A common design goal is to find a waveform $p(t)$ that minimizes the spectral occupation of the communication scheme subject to the constraint that the filters are self-orthogonal at translations of integer multiples of T . The orthogonality constraint ensures that there is no ISI in a distortionless channel and that the receiver filter neither amplifies nor correlates the white noise component of the external interference. If the channel is distortionless, then $c[k] = r_{\phi_s\phi_r}(kT/N)$. Therefore, by examining (4), for the DSP-based scheme in Fig. 2, a) there is no ISI in a distortionless channel if $\sum_q r_{\phi_s\phi_r}(qT/N)r_g[q - Nn] = \delta[n]$, where $\delta[n]$ denotes the Kronecker delta, and b) there is no amplification nor correlation of the white noise component of $\eta_c(t)$ if $\sum_q r_{\phi_s\phi_r}(qT/N)r_g[q - Nn] = \delta[n]$. In applications in which both $r_{\phi_s\phi_r}(qT/N)$ and $r_{\phi_r\phi_r}(qT/N)$ are sufficiently close to $\delta[q]$, the orthogonality constraint can be imposed directly on the filter [see (5a) and (9a)].

The spectral occupation of a communication scheme is usually measured in terms of its (time-averaged) power spectrum. For the simple case of stationary white data with zero mean and variance v_d , the power spectrum of $s_c(t)$ is $S_{s_c}(F) = (v_d/T)|P(F)|^2 = (v_d/T)|\Phi_s(F)|^2|G(e^{j2\pi FT/N})|^2$, where $P(F)$, $\Phi_s(F)$, and $G(e^{j2\pi f})$ are the Fourier transforms of $p(t)$, $\phi_s(t)$, and $g[k]$, respectively, and we have used F to denote frequency in a continuous-time setting. One commonly used measure of the spectral occupation of a communication scheme is the 100 γ % energy bandwidth of $s_c(t)$ denoted $B_{c,\gamma}$ [3], [4], [13], [21]. It is defined to be the smallest β_c such that

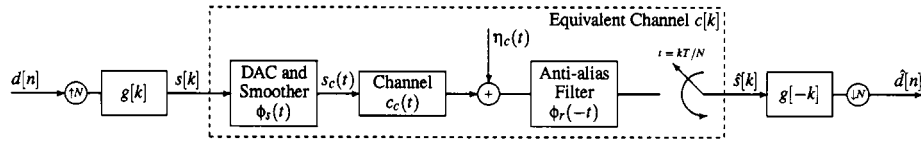


Fig. 2. Multirate digital signal processing implementation of the scheme in Fig. 1.

$\int_0^{\beta c} S_{s_c}(F) dF \geq \gamma \int_0^\infty S_{s_c}(F) dF$. If $|\Phi_s(F)|$ is sufficiently close to the ideal filter of bandwidth $N/(2T)$, then

$$\frac{\int_0^{\beta c} S_{s_c}(F) dF}{\int_0^\infty S_{s_c}(F) dF} \approx \frac{\int_0^{\beta c N/T} |G(e^{j2\pi f})|^2 df}{\int_0^{1/2} |G(e^{j2\pi f})|^2 df}$$

and hence, $B_{c,\gamma} \approx B_\gamma N/T$, where B_γ is the 100 γ % *energy bandwidth* of $g[n]$, which is defined to be the smallest β such that $\int_0^\beta |G(e^{j2\pi f})|^2 df \geq \gamma \int_0^{1/2} |G(e^{j2\pi f})|^2 df$. The term $|G(e^{j2\pi f})|^2$ is known as the *power spectrum* of $g[k]$. For convenience, we will often normalize the filter energy so that $\sum_{k=0}^{L-1} |g[k]|^2 = 2 \int_0^{1/2} |G(e^{j2\pi f})|^2 df = 1$. Finally, we observe that the Fourier transform of the autocorrelation $r_g[m]$ satisfies $R_g(e^{j2\pi f}) = r_g[0] + 2 \sum_{m=1}^{L-1} r_g[m] \cos(2\pi m f) = |G(e^{j2\pi f})|^2$.

III. A FEASIBILITY PROBLEM

In this section, we introduce the fundamentals of our design framework by studying various formulations of the following simple feasibility problem for the filter $g[k]$ in Fig. 2: *For a given γ, B, N , and L , either find an orthogonal filter $g[k]$ of length at most L with a 100 γ % energy bandwidth less than or equal to B or show that none exists.* If we formulate this problem directly in terms of the filter coefficients, the orthogonality and bandwidth constraints are

$$\sum_{k=\ell N}^{L-1} g[k]g[k-N\ell] = \delta[\ell], \quad \ell = 0, 1, \dots, \lfloor (L-1)/N \rfloor \quad (5a)$$

$$\int_0^B |G(e^{j2\pi f})|^2 df \geq \gamma/2 \quad (5b)$$

respectively, where $\lfloor x \rfloor$ denotes the greatest integer $\leq x$. Unfortunately, both these constraints are nonconvex in the parameters $g[k]$. As a result, determining an answer to the feasibility problem may be complicated by the presence of local minima, particularly when we wish to determine that no solutions exist. However, using relationships from Section II, we can parameterize the problem in terms of the autocorrelation $r_g[m]$, resulting in the linear constraints in (9a) and (9b) and the additional linear inequality constraint

$$R_g(e^{j2\pi f}) \geq 0, \quad \text{for all } f \in [0, 1/2]. \quad (6)$$

This additional constraint is a necessary and sufficient condition for $r_g[m]$ to be factorizable (by the Féjer–Riesz theorem [30]). The linearity of these constraints ensures that the (autocorrelation) design problem is a linearly-constrained convex feasibility problem. Once a feasible autocorrelation has been found (via any of the standard linear programming techniques [31], including those based on interior point methods), a feasible filter

can be found by spectral factorization. (An informative review of spectral factorization techniques appears in [19].) Furthermore, duality results can be exploited to provide a “certificate” (i.e., verification) of infeasibility when there is no feasible solution. Unfortunately, the non-negativity constraint in (6) is a semi-infinite constraint in that it must be satisfied for all values of $f \in [0, 1/2]$. Although that constraint can be handled using discretization techniques [14], such an approach may lead to overly conservative designs and can be rather awkward numerically in our application [8].

We now apply the Positive-Real Lemma to transform the semi-infinite constraint in (6) into a finite-dimensional constraint with some auxiliary variables and, hence, avoid the above-mentioned difficulties. The lemma will employ the well-known concepts of controllability and detectability of a state space realization [32], [33].

Lemma 1 (Positive-Real Lemma): Let $H(z)$ be a (stable) real rational function with its poles (if any) inside the unit circle. Suppose that $H(\infty)$ is finite and that $H(z)$ admits a controllable and detectable state-space realization $H(z) = d + \mathbf{c}(z\mathbf{I} - \mathbf{A})^{-1}\mathbf{b}$, with $d \geq 0$. Then, $H(e^{j2\pi f}) + H(e^{-j2\pi f}) \geq 0$ for all $f \in \mathbb{R}$ if and only if there exists a real symmetric matrix \mathbf{P} such that

$$\mathbf{M}(\mathbf{P}) \triangleq \begin{bmatrix} \mathbf{P} - \mathbf{A}^T \mathbf{P} \mathbf{A} & \mathbf{c}^T - \mathbf{A}^T \mathbf{P} \mathbf{b} \\ (\mathbf{c}^T - \mathbf{A}^T \mathbf{P} \mathbf{b})^T & 2d - \mathbf{b}^T \mathbf{P} \mathbf{b} \end{bmatrix} \geq 0. \quad (7)$$

This lemma appears in a variety of forms in the literature (see [15], [18], [32], [34], and references therein). The present form (based on [34]) is chosen because it requires only detectability (rather than observability) of the realization of $H(z)$ and because the symmetric matrix \mathbf{P} is unconstrained. This allows us to avoid redundant constraints in Formulation 1. Using the “stability” of $H(z)$ and a result of Lyapunov [33], it can be shown that all symmetric matrices \mathbf{P} satisfying (7) are positive semidefinite: a result that will be exploited in Lemma 2.

Since $R_g(z) = 1 + \sum_{m=1}^{L-1} r_g[m](z^m + z^{-m})$, the realization $H(z) = d + \mathbf{c}(z\mathbf{I} - \mathbf{A})^{-1}\mathbf{b}$ with

$$\mathbf{A} = \begin{bmatrix} \mathbf{0} & \mathbf{I}_{L-2} \\ 0 & \mathbf{0} \end{bmatrix}, \quad \mathbf{b} = \begin{bmatrix} \mathbf{0} \\ 1 \end{bmatrix} \quad (8a)$$

$$\mathbf{c} = [r_g[L-1] \quad \tilde{\mathbf{r}}_g], \quad d = 1/2 \quad (8b)$$

and $\tilde{\mathbf{r}}_g = [r_g[L-2], r_g[L-3], \dots, r_g[1]]$ satisfies the conditions of Lemma 1. (If $r_g[L-1] \neq 0$, the realization is observable.) Using this realization, the feasibility problem can be cast as the following formulation.

Formulation 1: Given γ, B, N , and L , either find $r_g[m], m = 0, 1, \dots, L-1$, and $\mathbf{P} = \mathbf{P}^T = \begin{bmatrix} \mathbf{p}_{11} & \mathbf{p}_{12} \\ \mathbf{p}_{12}^T & \mathbf{p}_{22} \end{bmatrix}$ with p_{22} being a scalar such that

$$r_g[\ell N] = \delta[\ell], \quad \text{for } \ell = 0, 1, \dots, \lfloor (L-1)/N \rfloor \quad (9a)$$

$$\frac{1}{\pi} \sum_{m=1}^{L-1} r_g[m] \sin(2\pi mB)/m \geq \gamma/2 - B \quad (9b)$$

$$\begin{bmatrix} \mathbf{P}_{11} & \mathbf{p}_{12} \\ \mathbf{p}_{12}^T & p_{22} \end{bmatrix} - \begin{bmatrix} 0 & \mathbf{0} \\ \mathbf{0} & \mathbf{P}_{11} \end{bmatrix} \begin{bmatrix} r_g[L-1] \\ \tilde{\mathbf{r}}_g^T - \mathbf{p}_{12} \\ 1 - p_{22} \end{bmatrix} \geq 0 \quad (9c)$$

or show that none exist.

Formulation 1 consists of linear constraints [(9a) and (9b)] and a linear matrix inequality (LMI) constraint (9c). Hence, it is a semidefinite feasibility problem [16] and can be solved in a highly efficient manner using interior point methods [17]. (Several generic SDP solvers are available, including the MATLAB-based SeDuMi package [35].) Semidefinite programming techniques have been applied to efficiently solve a number of other engineering problems, including many in control [36], [37] and a few in signal processing [20], [38], [39]. We point out that in Formulation 1, the orthogonality constraint (5a) is enforced precisely by (9a) and that both the bandwidth constraint (5b) and the non-negativity constraint (6) are enforced precisely [by (9b) and (9c), respectively], without discretization in frequency. In contrast, enforcing a simple sampled version of the non-negativity constraint (6) in a linear programming formulation involves a compromise between the number of discretization points N_d (i.e., the number of constraints) and the conservativity factor ϵ_{N_d} , which is chosen such that $R_g(e^{j2\pi i/(2N_d)}) \geq \epsilon_{N_d}$, $i = 0, 1, \dots, N_d - 1$ guarantees that $R_g(e^{j2\pi f}) \geq 0$ for all $f \in [0, 1/2]$. (A “rule of thumb” is to choose $N_d \approx 15L$, [19].) The concession for the precision of Formulation 1 is the LMI and the additional $(L-1)(L-2)/2$ variables in the symmetric half of \mathbf{P} . Although the resulting SDP may require a greater computational effort than a (conservative) sampled linear program with a moderate value of N_d , the total solution time in solving the SDP is still quite acceptable (e.g., a couple of minutes on a standard personal computer).

By solving Formulation 1, we obtain a feasible autocorrelation or a certificate of infeasibility when there is no feasible autocorrelation. In the feasible case, a feasible filter could then be found by spectral factorization (using any of the methods surveyed in [19]). An advantage of Formulation 1 is that it can be simply modified to produce the minimum-phase [18] spectral factor directly, without the need for auxiliary spectral factorization, using the following lemma (collected from results in [18]).

Lemma 2: Assume the same setting as Lemma 1 and that $\mathbf{M}(\mathbf{P}) \geq 0$ for some positive semidefinite matrix \mathbf{P} . Then, there exists a minimal solution $\bar{\mathbf{P}}$ to $\mathbf{M}(\mathbf{P}) \geq 0$, i.e., $\forall \mathbf{P} = \mathbf{P}^T$ such that $\mathbf{M}(\mathbf{P}) \geq 0$, $\mathbf{P} \geq \bar{\mathbf{P}}$. Let $d_w = \sqrt{2d - \mathbf{b}^T \bar{\mathbf{P}} \mathbf{b}}$, and let $\mathbf{c}_w = (\mathbf{c}^T - \mathbf{A}^T \bar{\mathbf{P}} \mathbf{b})/d_w$. Then, $W(z) = d_w + \mathbf{c}_w(z\mathbf{I} - \mathbf{A})^{-1} \mathbf{b}$ is the minimum phase spectral factor (up to a sign ambiguity) of $H(z) + H(z^{-1})$.

We can obtain $\bar{\mathbf{P}}$ by replacing Formulation 1 by the following semidefinite program.

Formulation 2: Given γ , B , N , and L , either find $r_g[m]$, $m = 0, 1, \dots, L-1$, and $\mathbf{P} = \mathbf{P}^T$ partitioned as in Formulation 1 achieving $\min \text{trace}(\mathbf{P})$ subject to (9), or show that none exist.

Once Formulation 2 has been solved, a feasible filter $g[k]$ can be found by direct substitution into Lemma 2, without auxiliary spectral factorization. In that case, $G(z) = d_g + \mathbf{c}_g(z\mathbf{I} - \mathbf{A})^{-1} \mathbf{b}$,

where \mathbf{A} and \mathbf{b} were given in (8), $d_g = \sqrt{1 - \bar{p}_{22}}$, and $\mathbf{c}_g = [r_g[L-1] \quad \tilde{\mathbf{r}}_g - \bar{\mathbf{p}}_{12}^T]/d_g$. Hence

$$g[k] = \begin{cases} \sqrt{1 - \bar{p}_{22}}, & k = 0 \\ [\tilde{\mathbf{r}}_g - \bar{\mathbf{p}}_{12}^T]_{L-1-k} / \sqrt{1 - \bar{p}_{22}}, & k = 1, 2, \dots, L-2 \\ r_g[L-1] / \sqrt{1 - \bar{p}_{22}}, & k = L-1 \end{cases} \quad (10)$$

where $[\mathbf{v}]_i$ denotes the i th element of a vector \mathbf{v} . We point out that if $r_g[m]$ is fixed, then Formulation 2 provides a convex optimization method for spectral factorization.

IV. SOME DESIGN PROBLEMS

In this section, we adapt the framework established in Section III to the solution of a number of pulse shaping filter design problems. We first discuss problems in which the spectral occupation is measured in terms of the percentage energy bandwidth. In Section IV-B, we will use alternative measures of bandwidth based on spectral masks, and in Section IV-C, we show how the characteristics of the smoothing and antialiasing filters can be incorporated into the designs.

A. Using the Percentage Energy Bandwidth

A natural extension to the feasibility problem studied in the previous section is to search for an orthogonal filter that provides the smallest 100 γ % energy bandwidth for a given length L and fraction γ . This problem can be phrased as follows.

Problem 1: For a given N , L , and γ , find a filter achieving $\min B$ over variables $r_g[m]$, $m = 0, 1, \dots, L-1$, $\mathbf{P} = \mathbf{P}^T$, and B subject to the constraints in (9).

For a fixed value of B , Problem 1 is the semidefinite feasibility problem in Formulation 1. Furthermore, it can be shown that (for $0 < \gamma < 1$), Formulation 1 will yield a positive result for $B \geq B^*$ and a negative result for $B < B^*$, where B^* is the solution to Problem 1. Therefore, B^* and the optimal autocorrelation $r_g^*[m]$ can be found using a bisection search on B , starting with lower and upper values of zero and one half, respectively. An optimal filter could then be found by any spectral factorization technique, including solving Formulation 2 given $B = B^*$ and $r_g[m] = r_g^*[m]$, and then applying (10). As an alternative, we could replace Formulation 1 by Formulation 2 at each stage of the bisection search so that (10) is immediately applicable, and an optimal filter is obtained directly. A property of many interior point methods for the solution of Formulations 1 and 2 is that they require about the same computational effort. Therefore, this alternative method remains efficient. We will refer to both these solution methods as *semidefinite programming based bisection search (SDP-BS)* methods. We demonstrate the application of Problem 1 in the following example.

Example 1: In this example, we design orthogonal filters to compete with a sampled and truncated implementation of the filter with a square-root cosine roll-off frequency response [40]. The roll-off factor was chosen to be $\alpha = 0.22$. (The same choice of filter was made for the “chip waveform” in the UMTS proposal [29].) We choose $N = 4$ and $L = 49$ so that the truncated root cosine roll-off filter remains approximately orthogonal. That filter has a 99% energy bandwidth of $B_{0.99} \approx 0.1351$. (Due to a fortuitous combination of sampling

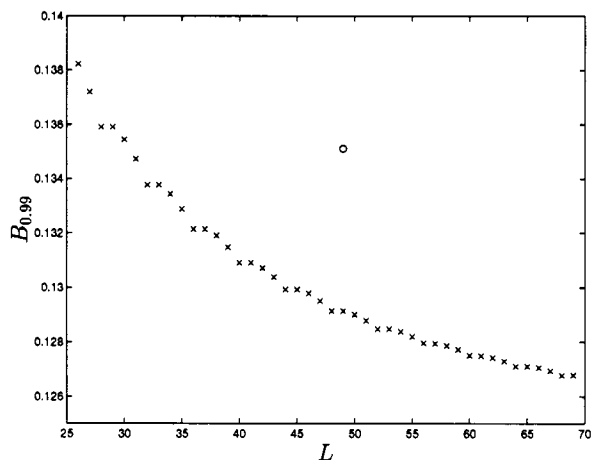


Fig. 3. Minimal achievable 99% energy bandwidth $B_{0.99}$ for an orthogonal filter of length L marked with \times 's (calculated in Example 1). The circle denotes the position of the (almost orthogonal) truncated root cosine roll-off filter with $\alpha = 0.22$ and $L = 49$.

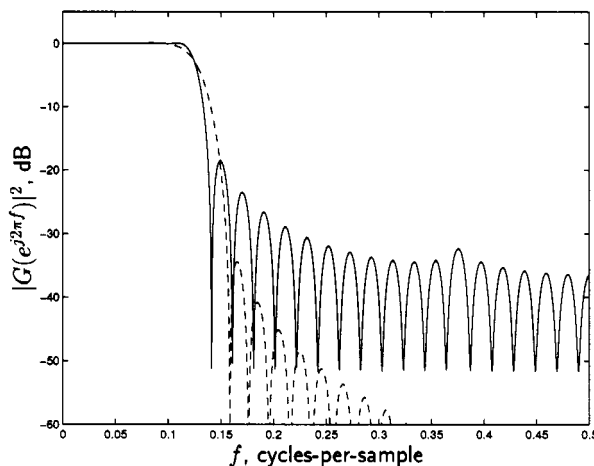
and truncation effects, this is a particularly good choice in the sense that this filter has better spectral decay than those of length $L = 48, 50,$ and 51 .) By solving Problem 1 for the same values of N and γ and using SeDuMi [35] to solve the SDP's, the minimum achievable $B_{0.99}$ with an orthogonal filter of length L can be determined. The resulting relationship is shown in Fig. 3. (The “ragged” but nonincreasing nature of this relationship is due to the orthogonality constraint and is not due to numerical error. In particular, the orthogonality constraint (9a) effectively removes the extra degree of freedom in filters of length $KN + 1$, for $K \in \mathbb{Z}$, over those of length KN by constraining it to be zero.) For $L = 49$, the minimum achievable $B_{0.99}$ is ≈ 0.1291 , which is a reduction of more than 4% over that of the truncated root cosine roll-off filter of the same length. The power spectra of these two length 49 filters are plotted in Fig. 4(a). Observe, however, that the reduced 99% energy bandwidth has come at the expense of higher “sidelobes.” We will address this issue in Section IV-B. In the $L = 49$ case, the feasibility problem at each stage of the bisection search was evaluated in under 2 min and 45 s on a 400-MHz PENTIUM II workstation. \square

Of course, a minimal $100\gamma\%$ energy bandwidth may not be the primary design criterion for a pulse shaping filter. For instance, we may wish to design an orthogonal filter that minimizes the delay in the received data that is required to ensure that the receiver filter is causal, subject to a constraint on the energy bandwidth.

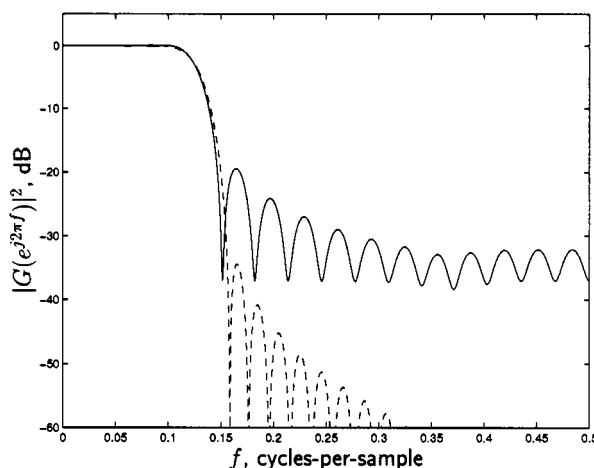
Problem 2: For a given $\gamma, N,$ and B , find a filter achieving $\min L$ over variables $r_g[m], m = 0, 1, \dots, L - 1, \mathbf{P} = \mathbf{P}^T,$ and $L \in \mathbb{Z}$ subject to the constraints in (9).

Problem 2 can also be solved by an SDP-BS method, but we must first obtain a feasible L . An iterative doubling technique will always produce a feasible L if one exists, but that search can often be reduced by using the designer's insight.

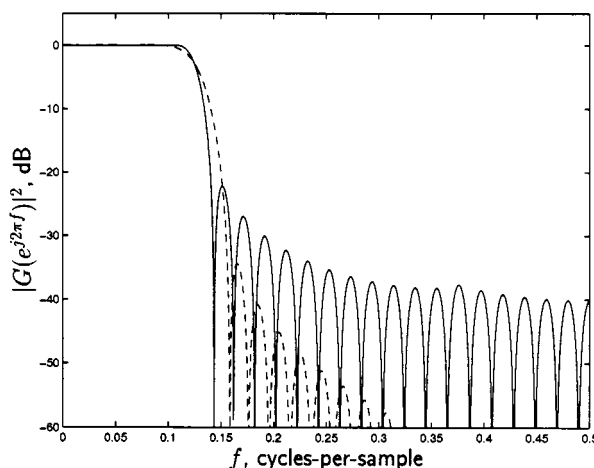
Example 2: By solving Problem 2, the smallest L such that there is an orthogonal filter with the same $B_{0.99}$ as the truncated root cosine roll-off filter of length 49 in Example 1 was found to be 31. This represents a substantial reduction in delay and computational requirements. (The problem at the last itera-



(a) Min. $B_{0.99}$ given $L = 49$.



(b) Min. L given $B_{0.99} = 0.1351$.



(c) Max. γ given $B_{\gamma} = 0.1351$ and $L = 49$.

Fig. 4. Relative power spectra (in decibels) of the designed filters (solid) and the root cosine roll-off filter (dashed) in Examples 1–3 [(a)–(c), respectively].

tion of the bisection search was evaluated in 11 s on a 400-MHz PENTIUM II workstation.) The power spectrum of the designed filter is plotted in Fig. 4(b). Note that as in Example 1 the designed filter has higher sidelobes than the root cosine roll-off filter. \square

In Problems 1 and 2, we minimized B and L , respectively. The obvious remaining problem is to maximize γ such that $B_\gamma \leq B$. (In the absence of the orthogonality constraint, the solution is a discrete-time prolate spheroidal function [41].) This problem is important when the channel bandwidth is (physically) constrained to B , and we wish to obtain the maximal spectral energy concentration in B . This problem has previously been formulated as a nonconvex optimization over $g[k]$ [3], [4], but it can also be formulated as the following (convex) SDP.

Problem 3: For a given N , L , and B , find a filter achieving $\max \gamma$ over variables $r_g[m]$, $m = 0, 1, \dots, L-1$, $\mathbf{P} = \mathbf{P}^T$ and γ subject to the constraints in (9).

Problem 3 is a semidefinite optimization problem (γ is a concave function of the parameters), and an optimal autocorrelation can be efficiently found from a single SDP (as distinct from the sequence of SDP's for the previous problems). An optimal filter can then be extracted by spectral factorization. That results in a *two-stage* method. Independently, but concurrently, with our work, Tuqan and Vaidyanathan [42] showed that the design of optimal orthogonal energy compaction filters for signal compression applications can also be formulated as Problem 3. (The corresponding semi-infinite linear programming formulation of the design of optimal orthogonal energy compaction filters appeared in [43].) In addition, they suggest replacing the objective in Problem 3 by

$$\max \gamma - \lambda \text{trace}(\mathbf{P}) \quad (11)$$

for some constant $\lambda > 0$ in order to find an optimal filter in a *single-stage* method. It can be shown that the solution \mathbf{P} of (11) is indeed the minimal \mathbf{P} so that (10) can be directly applied. Unfortunately, for any positive λ , (11) is not equivalent to the objective in Problem 3. Although a continuity argument suggests that the the optimal solution sets for the two problems are close for sufficiently small λ , the choice of λ appears to be rather *ad hoc*. (The choice $\lambda = 10^{-6}$ is suggested in the examples in [42].) If an appropriate value for λ is difficult to determine, the two-stage method may be more appropriate.

Example 3: By solving Problem 3 with $B = 0.1351$, we can find an orthogonal filter of length 49 that has the maximal spectral energy concentration within the 99% energy bandwidth of the truncated root cosine roll-off filter from Example 1. That optimal filter has 99.76% of its energy within that bandwidth. (The solution was obtained in under 3 min and 19 s on a 400-MHz PENTIUM II workstation.) The power spectrum of the designed filter is plotted in Fig. 4(c) from which it is clear that increase in γ has been achieved at the price of higher sidelobes. (Note that the sidelobes of the designed filter in Fig. 4(c) are more than 3 dB below those in Fig. 4(a).) \square

B. Using Spectral Mask-Based Measures of Bandwidth

By choosing the energy bandwidth as our design criterion, we lose control over the actual spectrum of the pulse shape, as is apparent from the high sidelobes in the designed filters in Fig. 4. This may require excessive guard bands between (uncoordinated) adjacent channels. In addition, many communication standards are specified in terms of a spectral mask that the transmitted signal must satisfy. Therefore, an alternative measure of

spectral occupation would be to constrain the power spectrum to lie within a given spectral mask, i.e.,

$$M_\ell(f) \leq R_g(e^{j2\pi f}) \leq M_u(f), \quad \text{for all } f \in [0, 1/2] \quad (12)$$

for some given mask $M_\ell(f)$ and $M_u(f)$. The mask constraints are linear in $r_g[m]$, and hence, the convexity of the previous feasibility problems is maintained. (The mask constraints are *not* convex in $g[k]$ unless the filter is constrained to have linear phase [19], [20]. It has been known for some time that a phase linearity constraint can lead to increased spectral occupation [4].) The mask constraint is a semi-infinite constraint, but it is less "critical" than that in (6) in that if (12) is violated and (6) is not, then a filter $g[k]$ with autocorrelation $r_g[m]$ does exist; it just fails to satisfy the mask. In practice, the mask constraint can be (conservatively) enforced using discretization techniques [14], [19], [20]. In many applications, filter masks are specified in terms of the relative magnitude of the power spectrum at different frequencies, usually on a logarithmic (decibel) scale. If we let $\rho_\ell(f)$ and $\rho_u(f)$ denote the lower and upper relative power spectrum bounds on $g[k]$, in decibels, then $M_\ell(f) = \zeta 10^{\rho_\ell(f)/10}$, for some $\zeta > 0$, and similarly for $M_u(f)$.

In Section III, we formulated the design of an orthogonal filter of a given length that has a certain percentage energy bandwidth as a semidefinite feasibility problem. The equivalent problem with a spectral mask bandwidth can also be formulated as a semidefinite feasibility problem.

Problem 4: Given $\rho_\ell(f)$, $\rho_u(f)$, N , and L , either find $r_g[m]$, $m = 0, 1, \dots, L-1$, $\mathbf{P} = \mathbf{P}^T$, and $\zeta > 0$ such that (9a) and (9c) are satisfied and that $\zeta 10^{\rho_\ell(f)/10} \leq R_g(e^{j2\pi f}) \leq \zeta 10^{\rho_u(f)/10}$ for all $f \in [0, 1/2]$, or show that none exist.

Problem 4 can be used as the subproblem in an SDP-BS method to find a minimal length filter for a given spectral mask, as we demonstrate in the following example.

Example 4: In this example, we design a filter to compete with the filter specified for the synthesis of the chip waveform in the IS95 standard [28]. Assuming an ideal smoothing filter, the standard requires a filter with a ± 1.5 -dB ripple in the passband $f \in [0, f_p]$ and 40-dB attenuation in the stopband $f \in [f_s, 1/2]$, where $f_p = 590/(1228.8N)$, and $f_s = 740/(1228.8N)$. The filter chosen in the standard has linear phase, $N = 4$, and $L = 48$, and hence, $f_p \approx 0.12$, and $f_s \approx 0.15$. Whereas that filter satisfies the spectral mask, it does not satisfy the orthogonality constraints (see Fig. 9 in Example 6). Hence, the IS95 filter can induce substantial "interchip" interference even when the physical channel is benign. Therefore, we seek a minimal length filter such that *both* the (relative) frequency response mask is satisfied *and* the filter is orthogonal. A globally optimal solution to this problem was found using an SDP-BS method based on Problem 4. The last SDP in the search was solved (using SeDuMi [35]) in just under 7 min and 20 s on a 400-MHz PENTIUM II workstation. The increase in computational time over that in Examples 1–3 is due to the nature of the bandwidth constraint. The energy bandwidth constraint is a single linear inequality in Examples 1–3, whereas the spectral mask constraint in this example is enforced by around 950 linear inequality constraints. The above procedure resulted in a length $L = 51$; therefore, orthogonality is achieved for the price of a mild increase

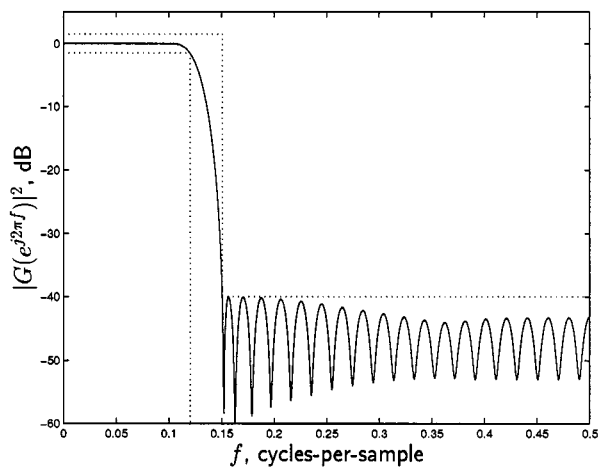
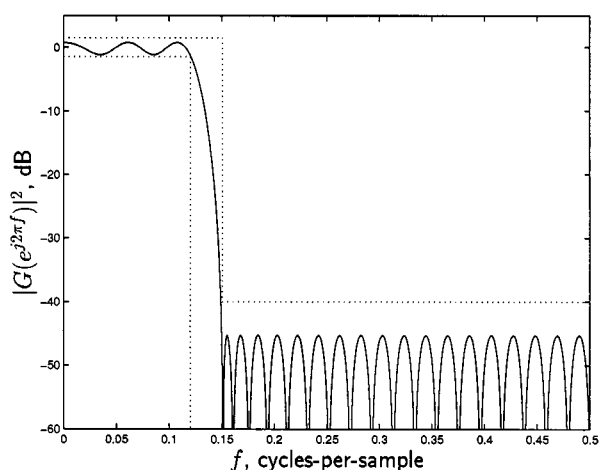

 (a) Designed orthogonal filter, $L = 51$.

 (b) IS95 filter (non-orthogonal), $L = 48$.

Fig. 5. Relative power spectra (in decibels) of the filters in Example 4 with the spectral mask from the IS95 standard.

in filter length. The frequency response of the designed filter is shown in Fig. 5(a). We observe that the equiripple characteristic associated with conventional linear-phase filters satisfying such masks does not extend to the case of minimum phase orthogonal filters. As can be seen from Fig. 5(b), the IS95 filter satisfies the spectral mask by a considerable margin. Using the same SDP-BS method, the minimal length filter satisfying both the mask *achieved* by the IS95 filter *and* the orthogonality constraints was found to have $L = 60$. As an aside, we point out that the shortest (approximately orthogonal) sampled and truncated square-root raised cosine filter that satisfies the mask specified in IS95 has a length $L = 108$ and a roll-off factor in a small interval around $\alpha = 0.135$.

To demonstrate the performance improvement due to the orthogonality of the designed filter, we evaluated the chip error rate (CER) for each filter for the case of binary chips transmitted with energy E over an additive white Gaussian noise channel with noise variance $N_0/2$ with sign detection (of the chips) at the receiver. This was done analytically (by using a formula from [1, p. 65]) and via simulation. Since the designed filters are orthogonal, their CER's are $(1/2) \operatorname{erfc}(\sqrt{E/N_0})$ [1], [2]. The results are plotted in Fig. 6. Note that for CER's of 10^{-3}

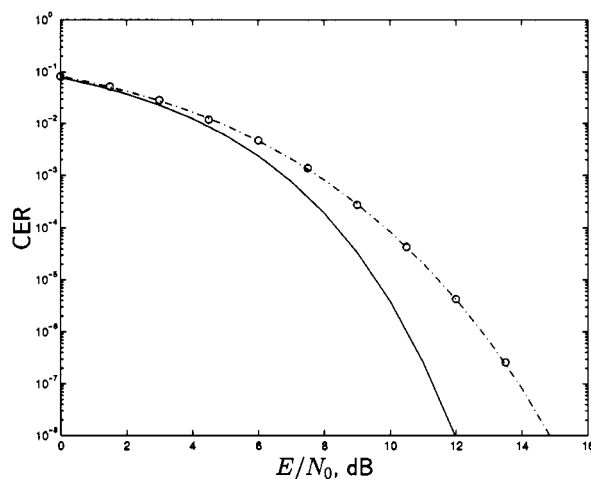


Fig. 6. Calculated (lines) and simulated (circles) chip error rates (CER) against signal-to-noise ratio for the filters in Example 4. Legend—Solid: designed filters; dash-dot and circle: IS95 filter.

and 10^{-6} , the signal-to-noise ratio gains are 1 dB and 2.4 dB, respectively. \square

In Example 4, we used Problem 4 to find a minimal-length orthogonal filter for a fixed spectral mask bandwidth, which is analogous to Problem 2. The corresponding problem of finding the minimal spectral mask bandwidth for a given L , which is analogous to Problem 1, is formulated in the next section.

C. Compensation for the Smoothing and Antialiasing Filters

In this subsection, we adjust the design of the pulse-shaping filter to compensate for the nonideal characteristics of the smoothing and antialiasing filters. In most implementations, these characteristics will be available to the designer with reasonable accuracy.

Using the analysis in Section II, we can eliminate any ISI in a distortionless channel if we ensure that $\sum_q r_{\phi_s \phi_r}(qT/N) r_g[q - Nn] = \delta[n]$. (Correlation of the white noise could be handled in a similar way.) By exploiting the symmetry of $r_g[m]$, this condition can be rewritten as

$$r_{\phi_s \phi_r}(nT) r_g[0] + \sum_{m=1}^{L-1} (r_{\phi_s \phi_r}(nT + mT/N) + r_{\phi_s \phi_r}(nT - mT/N)) r_g[m] = \delta[n]. \quad (13)$$

For complete ISI cancellation, this set of linear equations must hold for all n . For general $\phi_s(t)$ and $\phi_r(t)$, that may lead to an overdetermined linear system. Fortunately, $\phi_s(t)$ and $\phi_r(t)$ are usually essentially time limited in practice, and hence, the dominant components of ISI can be cancelled by enforcing (13) for appropriate values of n clustered around the origin. In order to provide normalization for $r_g[m]$ and to leave some freedom in $r_g[m]$ so that other constraints can be satisfied, we will enforce (13) for $n = 0$ and N_{ISI} values of n , where $N_{\text{ISI}} < L - 1$. The choice $N_{\text{ISI}} = \lfloor (L - 1)/N \rfloor$ will ensure the same number of equality constraints on $r_g[m]$ as there were in (9a). We note that if $\phi_s(t) = \phi_r(t)$, then using the resulting symmetry of $r_{\phi_s \phi_r}(\tau)$, we only need to consider non-negative values of n in (13). In that case, twice as many ISI terms can be cancelled.

In Formulation 1, we enforced an energy bandwidth constraint on the filter via the linear constraint on $r_g[m]$ in (9b). If, instead, we wish to enforce the energy bandwidth constraint directly on $s_c(t)$, (9b) can be replaced by $2 \sum_{m=1}^{L-1} (v_m - \gamma w_m) r_g[m] \geq \gamma w_0 - v_0$, where $v_m = \int_0^{B_c T/N} |\Phi_s(fN/T)|^2 \cos(2\pi m f) df$, $w_m = \int_0^{1/2} |\Phi_s(fN/T)|^2 \cos(2\pi m f) df$, and B_c is the energy bandwidth of $s_c(t)$. This constraint remains linear in $r_g[m]$ or γ , and hence, a filter that minimizes L or maximizes γ can be found in an analogous way to its idealized version (Problems 2 and 3, respectively). Furthermore, for a typical $\Phi_s(F)$, a filter that minimizes B_c can be found by an SDP-BS method once we have found a feasible B_c (using, say, an iterative doubling scheme). Absolute magnitude mask constraints of the form $M_{c,\ell}(F) \leq S_{s_c}(F) \leq M_{c,u}(F)$ can also be imposed on $s_c(t)$ simply by choosing $M_\ell(f) = TM_{c,\ell}(fN/T)/(v_d |\Phi_s(fN/T)|^2)$ and $M_u(f) = TM_{c,u}(fN/T)/(v_d |\Phi_s(fN/T)|^2)$ in (12). (Here, we have implicitly assumed that $\Phi_s(fN/T)$ is nonzero for $f \in [0, 1/2]$. All practical smoothing filters have this property.) The case of a relative spectral mask can be handled in an analogous manner.

We now show how to find the minimal achievable bandwidth in the sense of a spectral mask on $s_c(t)$ subject to the cancellation of the dominant ISI components. This is analogous to Problem 1 but with a spectral mask measure of bandwidth and compensation for the smoothing and antialiasing filters. For simplicity, we consider a relative spectral mask of the standard lowpass type used in the IS95 standard (and in Example 4), that is, with natural notation

$$\rho_{c,\ell}(F) = \begin{cases} \Delta_1, & \text{for } 0 \leq |F| \leq F_p \\ -\infty, & \text{for } |F| > F_p \end{cases}$$

$$\rho_{c,u}(F) = \begin{cases} \Delta_0, & \text{for } 0 \leq |F| < F_s/ \\ \Delta_2, & \text{for } |F| \geq F_s. \end{cases}$$

In that case, the problem can be formulated as follows.

Problem 5: Given $F_p, \Delta_0, \Delta_1, \Delta_2, \phi_s(t), \phi_r(t), T, N, L$, and $N_{\text{ISI}} < L - 1$, find a filter achieving $\min F_s$ over variables $r_g[m], m = 0, 1, \dots, L - 1, \mathbf{P} = \mathbf{P}^T, \zeta$, and F_s subject to $\zeta > 0, F_s > 0$, (13) for $n = 0$, and N_{ISI} other values of n chosen according to the characteristics of $r_{\phi_s \phi_r}(\tau)$, (9c), and

$$\zeta M_\ell(f) \leq R_g(e^{j2\pi f}) \leq \zeta M_u(f), \quad \text{for all } f \in [0, 1/2] \quad (14)$$

where $M_\ell(f) = 10^{\rho_{c,\ell}(fN/T)/10} / |\Phi_s(fN/T)|^2$, and $M_u(f)$ is defined similarly.

For a fixed value of F_s , Problem 5 is a semidefinite feasibility problem in variables $r_g[m], \mathbf{P}$, and ζ . Furthermore, the minimal F_s can be found by an SDP-BS method once we have found a feasible F_s .

Example 5: We now find the relationship between the minimal stopband edge and the length of the pulse shaping filter for the spectral mask in the IS95 standard, subject to the elimination of interchip interference in a distortionless channel. Minimizing the stopband edge minimizes the frequency separation required between an IS95 scheme and an adjacent occupant of the spectrum. (The benefit is twofold if the adjacent occupant is also operating an IS95 scheme with a minimal stopband edge.) We choose $N = 4$ and assume that the chip sequence is white and that the smoothing and antialiasing filters $\phi_s(t)$ and

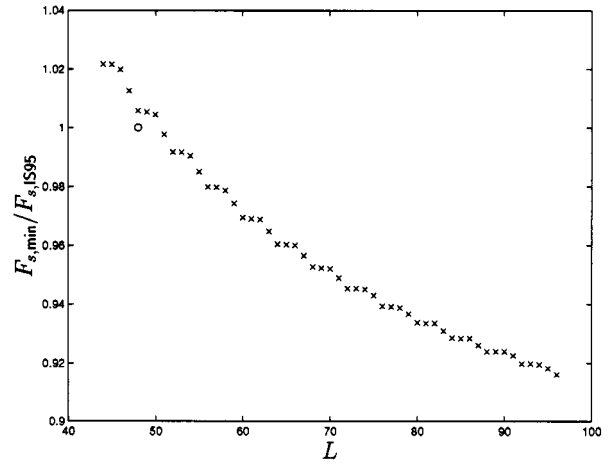


Fig. 7. Ratio of minimal achievable stopband edge $F_{s,\min}$ to the stopband edge in IS95 $F_{s,\text{IS95}}$ for an orthogonal waveform generated from a filter of length L , marked with \times 's (calculated in Example 5). The circle denotes the position of the (nonorthogonal) waveform generated from the filter in the IS95 standard.

$\phi_r(t)$ have been chosen to be root cosine roll-off filters with respect to T_c/N , with roll-off factor $\alpha = 0.5$. In that case, with $N_{\text{ISI}} = \lfloor (L - 1)/N \rfloor$, (13) collapses to (9a). In Fig. 7, we plot the variation of the ratio of the minimal stopband edge to the stopband edge chosen in the IS95 standard against filter length. Note that for $L = 96$, the stopband edge has been reduced by 9.16%. The power spectrum of the resulting waveform $p(t) = \sum_k g[k] \phi_s(t - kT_c/N)$ is plotted in Fig. 8 along with that generated by the IS95 filter with the same $\phi_s(t)$. \square

In Example 5, we found the most spectrally efficient waveform for a pulse shaping filter of a given length, where spectral efficiency was measured by F_s . Alternatively, we could fix the spectral mask and measure spectral efficiency as the maximal symbol rate $1/T$ such that the spectral mask is satisfied. (This problem is different from that in Problem 5 because adjusting T changes both the passband and stopband edges of the spectral mask on $g[k]$.) Although it is again true that for a fixed T we obtain a semidefinite feasibility problem, there may be disjoint intervals of T for which the new problem is feasible. Hence, a simple bisection search may not find the globally minimal T . Fortunately, more sophisticated, but less efficient, searches can be used instead. As an example, for the scenario in Example 5 and a filter length of $L = 96$, the chip rate of an IS95 scheme can be increased by 9.11% while maintaining the spectral mask and orthogonality.

V. ROBUSTNESS TO TIMING ERROR

In many communications applications, there may be significant timing "jitter" on the sampler at the receiver. That is, with reference to Fig. 2, the samples are taken at $t = kT/N + \epsilon_k$, where $-T/(2N) < \epsilon_k \leq T/(2N)$ rather than $t = kT/N$. Indeed, in some cases, timing jitter may be the dominant source of ISI. In this section, we show that the design of a filter that is maximally robust to timing error in a mean square error sense can be formulated as an SDP.

To model and analyze the case where timing error is the dominant source of ISI, we can consider the channel to be distortion-

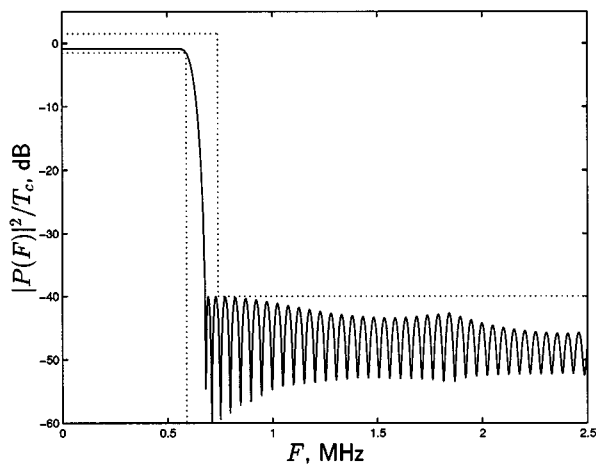
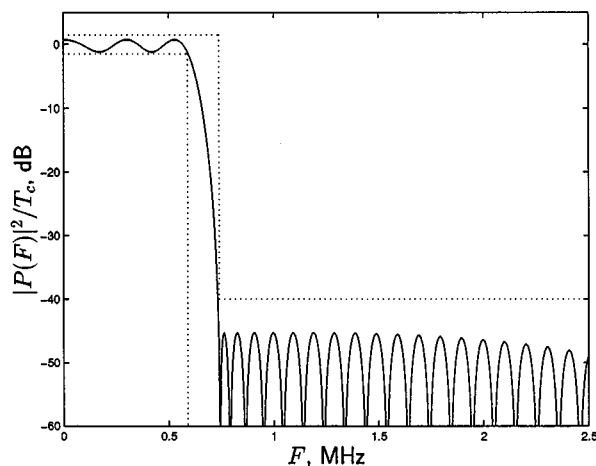
(a) Designed (orthogonal) waveform, $L = 96$ (b) IS95 waveform (non-orthogonal), $L = 48$.

Fig. 8. Relative power spectra (in decibels) of two of the waveforms in Example 5, with the spectral mask from the IS95 standard.

less. If ϵ_k varies slowly, then $\hat{s}[k] \approx \sum_m c_\epsilon[k-m]s[m] + \eta[k]$, where $\epsilon_k \approx \epsilon$, $c_\epsilon[k] \triangleq r_{\phi_s, \phi_r}(kT/N + \epsilon)$, and $\eta[k] = \int \phi_r(t - kT/N - \epsilon)\eta_c(t) dt$. For that model

$$\begin{aligned} \hat{d}[n] - d[n] &= \sum_i \left(\sum_p c_\epsilon[p]r_g[p + Ni] - \delta[i] \right) d[n+i] \\ &\quad + \sum_k g[k - Nn]\eta[k]. \end{aligned} \quad (15)$$

If the data is stationary and white with zero mean and variance v_d and the channel noise $\eta_c(t)$ is stationary and white with zero mean and variance v_{η_c} and is not correlated with the data, then for a given ϵ , the mean square error (MSE) in the data estimate (normalized by v_d) is

$$\begin{aligned} c_\epsilon^2 &\triangleq E\{(\hat{d}[n] - d[n])^2\} \\ &= \sum_i \left(\sum_p c_\epsilon[p]r_g[p + Ni] - \delta[i] \right)^2 \\ &\quad + \frac{1}{v_\rho} \sum_m r_{\phi_r, \phi_r}(mT/N)r_g[m] \end{aligned} \quad (16)$$

where $v_\rho = v_d/v_{\eta_c}$ is the ‘‘signal-to-noise ratio.’’ Hence, the average MSE is

$$\langle c_\epsilon^2 \rangle = \int_{-\frac{T}{2N}}^{\frac{T}{2N}} p_E(\epsilon)c_\epsilon^2 d\epsilon \quad (17)$$

where $p_E(\epsilon)$ is the probability density function (pdf) for ϵ (at the given SNR). (In deriving (17), we have implicitly assumed that the timing error is independent of the data and the white noise.) As shown in the Appendix, the average MSE can be rewritten as

$$\langle c_\epsilon^2 \rangle = \mathbf{r}_g^T \mathbf{Q} \mathbf{r}_g + \mathbf{l}^T \mathbf{r}_g + 1 \quad (18)$$

where $[\mathbf{r}_g]_m = r_g[m]$, $0 \leq m \leq L-1$, and the vector $\mathbf{l} = \mathbf{l}_{\eta_c}/v_\rho - 2\mathbf{l}_d$. Here, the elements of \mathbf{Q} and \mathbf{l}_d depend on $c_\epsilon[k]$ and $p_E(\epsilon)$, and those of \mathbf{l}_{η_c} depend on $r_{\phi_r, \phi_r}(mT/N)$. By its very nature, $\langle c_\epsilon^2 \rangle \geq 0$ for all \mathbf{r}_g , and therefore, the expression in (18) is a convex quadratic function of $r_g[m]$. Hence, \mathbf{Q} is a positive semidefinite matrix, and there is an $L \times \text{rank}(\mathbf{Q})$ matrix \mathbf{L} such that $\mathbf{Q} = \mathbf{L}\mathbf{L}^T$.

A natural objective is to minimize the average MSE, but that objective is a quadratic function and, hence, is not expressed as an SDP. To cast the minimization of $\langle c_\epsilon^2 \rangle$ as a (convex) ‘‘symmetric cone’’ program (of which SDP’s are a special case), we observe that $\langle c_\epsilon^2 \rangle \leq \sigma + \mathbf{l}^T \mathbf{r}_g + 1$ for some $\sigma \in \mathbb{R}$, if and only if

$$\|\mathbf{L}^T \mathbf{r}_g\|_2^2 \leq \sigma. \quad (19)$$

Therefore a filter that generates a waveform that a) satisfies a (general) relative spectral mask on $s_c(t)$ and b) provides maximal robustness to timing error can be found as the solution of the following ‘‘symmetric cone programme.’’

Problem 6: Given $\rho_{c, \ell}(F)$, $\rho_{c, u}(F)$, $\phi_s(t)$, $\phi_r(t)$, v_ρ , $p_E(\epsilon)$, T , N and L , find a filter achieving

$$\min \sigma + \mathbf{l}^T \mathbf{r}_g \quad (20)$$

over variables $r_g[m]$, $m = 0, 1, \dots, L-1$, $\mathbf{P} = \mathbf{P}^T$, σ and $\zeta > 0$ subject to (9c), (14), (19) and

$$\begin{aligned} r_{\phi_s, \phi_r}(0)r_g[0] &+ \sum_{m=1}^{L-1} (r_{\phi_s, \phi_r}(mT/N) \\ &+ r_{\phi_s, \phi_r}(-mT/N))r_g[m] = 1 \end{aligned} \quad (21)$$

where $\mathbf{l} = \mathbf{l}_{\eta_c}/v_\rho - 2\mathbf{l}_d$, \mathbf{L} is such that $\mathbf{Q} = \mathbf{L}\mathbf{L}^T$, and \mathbf{Q} , \mathbf{l}_d and \mathbf{l}_{η_c} are given in (22)–(24) in the Appendix, respectively.

Here, we have normalized $r_g[m]$ in (21) so that there is a unit gain for the desired data symbol in the absence of timing error. Problem 6 consists of a linear objective (20), subject to a linear equality constraint (21), linear inequality constraints (14), a linear matrix inequality (9c) and a rotated second-order cone [44] constraint (19). Hence the optimal autocorrelation can be efficiently found using tools for linear optimization over (certain) symmetric cones, such as SeDuMi [35]. An optimal filter can be found using either of the one-stage or two-stage methods, as discussed after Problem 3.

As one would expect, the optimal filter for Problem 6 is dependent on the SNR. If the SNR varies, a filter which minimizes the worst-case MSE over a range of SNR’s, or the expected MSE over a distribution of SNR’s, can often be found by solving Problem 6 for modified values of \mathbf{Q} and \mathbf{l} . Furthermore, if we

are able to design $\phi_r(t)$ so that it is self-orthogonal and $\phi_s(t)$ so that it is mutually orthogonal to $\phi_r(t)$, then (21) reduces to $r_g[0] = 1$, (18) reduces to $\langle e_c^2 \rangle = \mathbf{r}_g^T \mathbf{Q} \mathbf{r}_g - 2\mathbf{l}_d^T \mathbf{r}_g + 1/v_\rho + 1$ and the optimal filter becomes independent of the SNR.

We point out there is no explicit orthogonality constraint in Problem 6. Instead, we trade some ISI in the case of perfect timing for improved robustness in the presence of timing error. (We can also trade ISI for satisfaction of the spectral mask.) However, in the absence of timing error, if $\phi_r(t)$ is self-orthogonal and $\phi_s(t)$ and $\phi_r(t)$ are mutually orthogonal, then $\langle e_c^2 \rangle = e_0^2 = \sum_{\ell=-K}^K (r_g[N\ell] - \delta[\ell])^2 + r_g[0]/v_\rho$, where $K = \lfloor (L-1)/N \rfloor$. In that case, (21) reduces to $r_g[0] = 1$ and a global minimizer of $\langle e_c^2 \rangle$ subject to (21) has $r_g[\ell N] = 0$ for $\ell = 1, 2, \dots, K$, which is precisely the orthogonality constraint in (9a). (Of course, the resulting $s_c(t)$ might not satisfy the spectral mask.)

Example 6: In this example, we design another filter to compete with the filter specified for the synthesis of the chip waveform in IS95 [28]. We choose the smoothing and anti-aliasing filters from Example 5 and consider an additive white Gaussian noise channel in which the receiver is subject to a slowly varying timing error ϵ with a (symmetric) triangular pdf on $|\epsilon| \leq T_c/(2N)$ that is independent of the SNR. (This pdf is a representative choice that generates severe timing jitter with the likelihood of a given timing offset decreasing with its size.) The filter of length $L = 96$ that provides maximal robustness to this timing error, subject to the spectral mask constraint on $s_c(t)$ from the IS95 standard, was found by solving Problem 6 (which is independent of the SNR in this case). The resulting autocorrelation function for the waveform $p(t)$ in (2) can be written as $r_{pp}(\tau) = \sum_m r_g[m] r_{\phi_s \phi_s}(\tau + mT_c/N)$ and is shown in Fig. 9. For comparison, Fig. 9 also contains $r_{pp}(\tau)$ for the IS95 filter and the orthogonal $L = 51$ filter from Example 4. The improved robustness to timing error of the newly designed filter is clear from the fact that $|r_{pp}(\tau)|$ is small in the neighborhood of $\tau = nT_c$, $n \neq 0$. That the IS95 filter generates significant interchip interference even in the absence of timing error is clear from the fact that $r_{pp}(nT_c) \neq 0$ for $n \neq 0$.

To demonstrate the performance improvement of the newly designed filter, we simulated the chip error rate for each filter in a modified version of the scenario in Example 4 in which the receiver is subject to slowly varying timing error with the above pdf. The resulting chip error rate curves are plotted in Fig. 10. Since the spectral mask constraints are quite "tight," a significant increase in the filter length was required in order to obtain an appreciable improvement in CER over the orthogonal $L = 51$ filter from Example 4. \square

VI. CONCLUSION

We have shown that the design of orthogonal pulse shapes for waveform coding can be formulated as a convex semidefinite program, and hence, globally optimal waveforms can be found in an efficient manner. The formulation was motivated by the observation that the deployment of baseband digital signal processors removes many of the physical constraints in analog

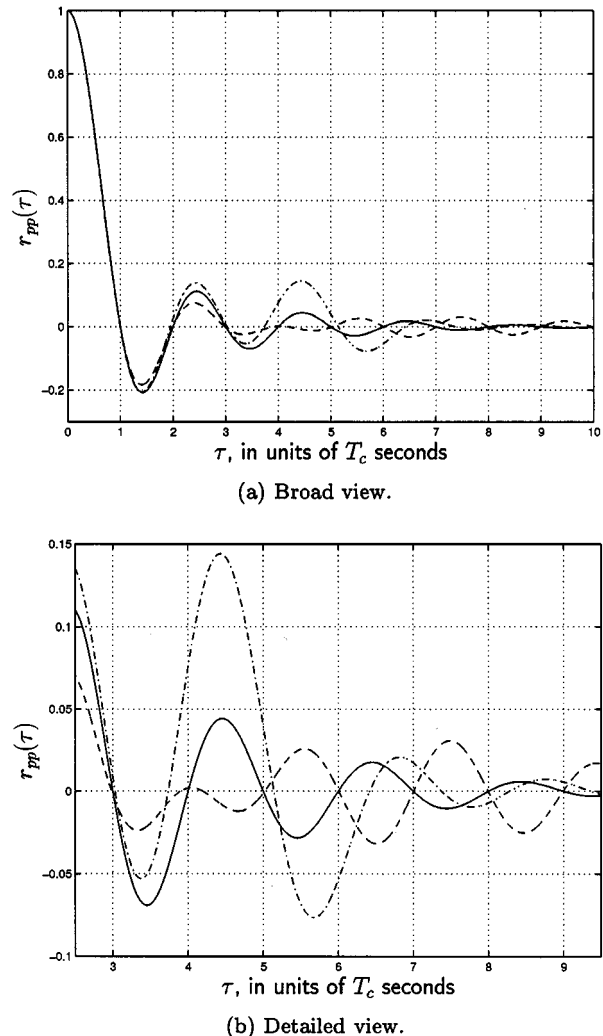


Fig. 9. Autocorrelations of the waveforms $p(t)$ for the filters in Example 6. Legend—Dashed: robust designed filter with $L = 96$; solid: orthogonal designed filter with $L = 51$ from Example 4; dash-dot: IS95 filter.

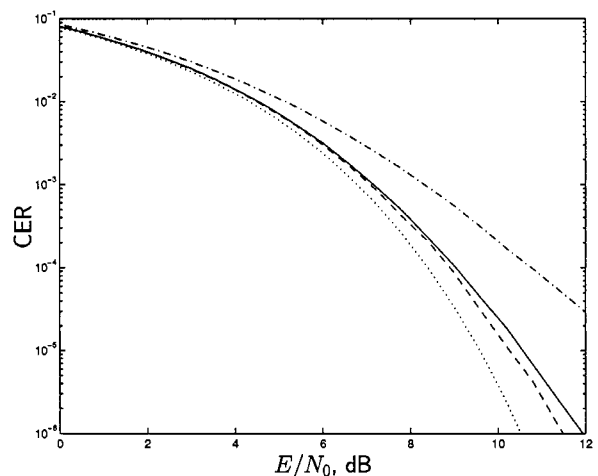


Fig. 10. Simulated chip error rates (CER) against signal-to-noise ratio for the filters in Example 6. Legend—Dashed: robust designed filter with $L = 96$; solid: orthogonal designed filter with $L = 51$ from Example 4; dash-dot: IS95 filter; dotted: calculated CER for an orthogonal chip waveform in the absence of timing error.

waveform coding applications and by a desire to exploit the resulting design freedom in an efficient manner. The formulation is based on the fact that many of the desirable properties of a coding waveform are actually properties of its autocorrelation. In particular, orthogonality is a linear constraint on the autocorrelation. We applied the Positive-Real Lemma to transform the rather awkward semi-infinite linear inequality constraint that appears in some current autocorrelation-based design methods into a finite linear matrix inequality. An advantage of this transformation is that the minimum-phase spectral factor and, hence, an optimal waveform, can be obtained directly from the output of the optimization routine.

Although there are many waveform designs that can be formulated in this way, we focussed on three of them, namely

- a) the minimal bandwidth for a given filter length;
- b) the minimal filter length for a given bandwidth;
- c) the maximal robustness to timing error.

Bandwidth was measured either in spectral energy concentration terms or with respect to a spectral mask. We demonstrated the effectiveness of our design technique by designing “chip waveforms” with superior performance to that of the chip waveforms specified in recent standards for CDMA-based mobile telecommunication systems. The efficiency of the design technique was demonstrated by the small computation times in the examples (compared with the times that would be required for reliable solution of the nonconvex formulations). We are currently exploring some reformulations of our design problems into forms that more closely match the internal structure of algorithms for the solution of the semidefinite programs. Initial experiments indicate that the computation times can be further reduced by factors of several tens for the problems considered in this paper.

Since the intersection of two convex sets is itself convex, many combinations of the problems considered in this paper can be solved using similar techniques. Furthermore, there are other pulse-shape characteristics that can also be incorporated into the semidefinite program. For instance, some recent work has indicated that robustness to frequency-selective fading can be measured in terms of a convex quadratic function of the autocorrelation [45]. The techniques of this paper can be easily extended to provide direct design of complex-valued pulse shaping filters (as distinct from separate design of the real and imaginary parts) now that generic SDP solvers that accommodate complex data are being introduced. The techniques may also be applicable to the design of some precoding schemes and in the design of multiplexing schemes in which the pulse-shaping filter for each user is obtained from a single prototype filter, e.g., OFDM. In addition, applications may appear in signal processing fields, such as the design of certain structured multirate filter banks and wavelet design, especially when phase linearity is not required. However, there are a few waveform characteristics that are important in some communications applications but are functions of the waveform itself, rather than its autocorrelation. For example, the strength of the cyclic autocorrelation coefficients of $s_c(t)$ and the magnitude of the envelope variation of $s_c(t)$. An interesting direction for future work is to examine ways in which such characteristics can be incorporated into the current design framework.

APPENDIX DERIVATION OF (18)

Expanding (16), we have that

$$\begin{aligned} \epsilon_c^2 &= \sum_{\ell, m} r_g[\ell] r_g[m] \sum_i c_\epsilon[\ell - Ni] c_\epsilon[m - Ni] \\ &\quad - 2 \sum_m r_g[m] c_\epsilon[m] + 1 \\ &\quad + \frac{1}{v_\rho} \sum_m r_g[m] r_{\phi_r \phi_r}(mT/N) \\ &= \check{\mathbf{r}}_g^T \check{\mathbf{Q}}_\epsilon \check{\mathbf{r}}_g + \left(\check{\mathbf{1}}_{\eta_c}^T / v_\rho - 2 \check{\mathbf{1}}_{d, \epsilon}^T \right) \check{\mathbf{r}}_g + 1 \end{aligned}$$

where $[\check{\mathbf{r}}_g]_m = r_g[m]$, $1 - L \leq m \leq L - 1$. Here, the matrix $\check{\mathbf{Q}}_\epsilon = \sum_j \mathbf{c}_{\epsilon, j} \mathbf{c}_{\epsilon, j}^T = \mathbf{C}_\epsilon \mathbf{C}_\epsilon^T$, with $[\mathbf{c}_{\epsilon, j}]_i = c_\epsilon[i - Nj]$ and $[\mathbf{C}_\epsilon]_{ij} = c_\epsilon[i - Nj]$ for $1 - L \leq i \leq L - 1$, and the vectors $[\check{\mathbf{1}}_{\eta_c}]_m = r_{\phi_r \phi_r}(mT/N)$ and $[\check{\mathbf{1}}_{d, \epsilon}]_m = c_\epsilon[m]$. Since $r_g[-m] = r_g[m]$, we have that

$$\check{\mathbf{r}}_g = \mathbf{T} \mathbf{r}_g = \begin{bmatrix} \mathbf{0} & \mathbf{J} \\ \mathbf{1} & \mathbf{0} \\ \mathbf{0} & \mathbf{I} \end{bmatrix} \mathbf{r}_g$$

where $[\mathbf{r}_g]_m = r_g[m]$, $m = 0, 1, \dots, L - 1$, and \mathbf{I} and \mathbf{J} are the identity and exchange matrices, respectively, of dimension $(L - 1) \times (L - 1)$. Substituting the above expressions into (17), we obtain (18), in which

$$\mathbf{Q} = \mathbf{T}^T \int p_E(\epsilon) \check{\mathbf{Q}}_\epsilon d\epsilon \mathbf{T} \quad (22)$$

$$\mathbf{l}_d = \mathbf{T}^T \int p_E(\epsilon) \check{\mathbf{1}}_{d, \epsilon} d\epsilon \quad (23)$$

$$\mathbf{l}_{\eta_c} = \mathbf{T}^T \check{\mathbf{1}}_{\eta_c} \quad (24)$$

where the integrals are taken elementwise. Since $\check{\mathbf{Q}}_\epsilon = \mathbf{C}_\epsilon \mathbf{C}_\epsilon^T$ is positive semidefinite, \mathbf{Q} is also positive semidefinite, and hence, $\mathbf{Q} = \mathbf{L} \mathbf{L}^T$ for some matrix \mathbf{L} .

REFERENCES

- [1] R. W. Lucky, J. Salz, and E. J. Weldon Jr., *Principles of Data Communications*. New York: McGraw-Hill, 1968.
- [2] B. Sklar, *Digital Communications. Fundamentals and Applications*. Englewood Cliffs, NJ: Prentice-Hall, 1988.
- [3] P. H. Halpern, “Optimal finite duration Nyquist signals,” *IEEE Trans. Commun.*, vol. COMM-27, pp. 884–888, June 1979.
- [4] P. R. Chevillat and G. Ungerboeck, “Optimum FIR transmitter and receiver filters for data transmission over band-limited channels,” *IEEE Trans. Commun.*, vol. COMM-30, pp. 1909–1915, Aug. 1982.
- [5] T. W. Parks and C. S. Burrus, *Digital Filter Design*. New York: Wiley, 1987.
- [6] P. P. Vaidyanathan, *Multirate Systems and Filter Banks*. Englewood Cliffs, NJ: Prentice-Hall, 1993.
- [7] K. Steiglitz, T. W. Parks, and J. F. Kaiser, “METEOR: A constraint-based FIR filter design program,” *IEEE Trans. Signal Processing*, vol. 40, pp. 1901–1909, Aug. 1992.
- [8] H. Samuelli, “On the design of optimal equiripple FIR digital filters for data transmission applications,” *IEEE Trans. Circuits Syst.*, vol. 35, pp. 1542–1546, Dec. 1988.
- [9] —, “On the design FIR digital data transmission filters with arbitrary magnitude specifications,” *IEEE Trans. Circuits Syst.*, vol. 38, pp. 1563–1567, Dec. 1991.

- [10] J. O. Coleman and D. W. Lytle, "Linear-programming techniques for the control of intersymbol interference with hybrid FIR/analog pulse shaping," in *Proc. IEEE Int. Conf. Commun.*, Chicago, IL, June 1992.
- [11] J. O. Coleman, "Linear-programming design of data-communication pulses tolerant of timing jitter or multipath," in *Proc. 5th Int. Conf. Wireless Commun.*, Calgary, Alta., Canada, July 1993.
- [12] O. Rioul and P. Duhamel, "A Remez exchange algorithm for orthonormal wavelets," *IEEE Trans. Circuits Syst. II*, vol. 41, pp. 550–560, Aug. 1994.
- [13] A. Said and J. B. Anderson, "Bandwidth-efficient coded modulation with optimized linear partial-response signals," *IEEE Trans. Inform. Theory*, vol. 44, pp. 701–713, Mar. 1998.
- [14] R. Hettich and K. O. Kortanek, "Semi-infinite programming: Theory, methods and applications," *SIAM Rev.*, vol. 35, no. 3, pp. 380–429, Sept. 1993.
- [15] L. Hitz and B. D. O. Anderson, "Discrete positive-real functions and their application to system stability," *Proc. Inst. Elect. Eng.*, vol. 116, no. 1, pp. 153–155, Jan. 1969.
- [16] L. Vandenberghe and S. Boyd, "Semidefinite programming," *SIAM Rev.*, vol. 31, no. 1, pp. 49–95, Mar. 1996.
- [17] Y. Ye, *Interior Point Algorithms: Theory and Analysis*. New York: Wiley, 1997.
- [18] B. D. O. Anderson, K. L. Hitz, and N. D. Diem, "Recursive algorithm for spectral factorization," *IEEE Trans. Circuits Syst.*, vol. CAS-21, pp. 742–750, Nov. 1974.
- [19] S.-P. Wu, S. Boyd, and L. Vandenberghe, "FIR filter design via spectral factorization and convex optimization," in *Appl. Comput. Contr., Signals, Circuits*, B. Datta, Ed. Boston, MA: Birkhauser, May 1999, vol. 1, ch. 5.
- [20] —, "FIR filter design via semidefinite programming and spectral factorization," in *Proc. IEEE Conf. Decision Contr.*, 1996, pp. 271–276.
- [21] K. H. Mueller, "A new approach to optimum pulse shaping in sampled systems using time-domain filtering," *Bell Syst. Tech. J.*, vol. 52, no. 5, pp. 723–729, May–June 1973.
- [22] F. Mintzer, "On half-band, third-band and N th band FIR filters and their design," *IEEE Trans. Acoust. Speech, Signal Processing*, vol. ASSP-30, pp. 734–738, Oct. 1982.
- [23] E. Panayirci and N. Tuğbay, "Optimum design of finite duration Nyquist signals," *Signal Process.*, vol. 7, pp. 57–64, 1984.
- [24] J. K. Liang, R. J. P. de Figueiredo, and F. C. Lu, "Design of optimal Nyquist, partial response, N th band, and nonuniform tap spacing FIR digital filters using linear programming techniques," *IEEE Trans. Circuits Syst.*, vol. CAS-32, pp. 386–392, Apr. 1985.
- [25] P. P. Vaidyanathan and T. Q. Nguyen, "Eigenfilters: A new approach to least-squares FIR filter design and applications including Nyquist filters," *IEEE Trans. Circuits Syst.*, vol. CAS-34, pp. 11–23, Jan. 1987.
- [26] T. Saramäki and Y. Neuvo, "A class of FIR Nyquist (N th-band) filters with zero intersymbol interference," *IEEE Trans. Circuits Syst.*, vol. 34, pp. 1182–1190, Oct. 1991.
- [27] B. Farhang-Boroujeny and G. Matthew, "Nyquist filters with robust performance against timing jitter," *IEEE Trans. Signal Processing*, vol. 46, pp. 3427–3431, Dec. 1998.
- [28] "Proposed EIA/TIA Interim Std. Wideband Spread Spectrum Digital Cellular Syst. Dual-Mode Mobile Station–Base Station Compatibility Std.," QUALCOMM, Inc., San Diego, CA, Tech. Rep. TR45.5, Apr. 1992.
- [29] "Universal Mobile Telecommun. Syst. (UMTS); UMTS Terrestrial Radio Access (UTRA); Concept Evaluation," Euro. Telecommun. Std. Inst., Sophia Antipolis, France, Tech. Rep. TR 101 146 v3.0.0 (1997-12), Dec. 1997.
- [30] A. Papoulis, *Signal Analysis*. New York: McGraw-Hill, 1977.
- [31] R. J. Vanderbei, *Linear Programming: Foundations and Extensions*. Boston, MA: Kluwer, 1996.
- [32] B. D. O. Anderson and S. Vongpanitlerd, *Network Analysis and Synthesis. A Modern Systems Theory Approach*. Englewood Cliffs, NJ: Prentice-Hall, 1973.
- [33] K. Zhou, J. C. Doyle, and K. Glover, *Robust and Optimal Control*. Upper Saddle River, NJ: Prentice-Hall, 1996.
- [34] B. Hassibi and T. Kailath, "A Krein space interpretation of the Kalman–Yakovitch–Popov lemma," *Inform. Syst. Lab., Stanford Univ., Stanford, CA*, [Online] Available: <http://www-isl.stanford.edu/hassibi/papers.html>, Aug. 1997.
- [35] J. F. Sturm, "SeDuMi: A MATLAB Toolbox for Optimization over Symmetric Cones. Software, User's Guide and Benchmarks," [Online] Available, <http://www.unimaas.nl/sturm/software/sedumi.html>, Aug. 1998.
- [36] S. Boyd, L. El Ghaoui, E. Feron, and V. Balakrishnan, *Linear Matrix Inequalities in System and Control Theory*. Philadelphia, PA: SIAM, 1994.
- [37] C. Scherer, P. Gahinet, and M. Chilali, "Multiobjective output-feedback control via LMI optimization," *IEEE Trans. Automat. Contr.*, vol. 42, pp. 896–911, July 1997.
- [38] H. Li and M. Fu, "A linear matrix inequality approach to robust H_∞ filtering," *IEEE Trans. Signal Processing*, vol. 45, pp. 2338–2350, Sep. 1997.
- [39] M. Fu, C. E. de Souza, and Z.-Q. Luo, "Finite horizon robust Kalman filter design," *IEEE Trans. Signal Processing*, submitted for publication [Online]. Available: <http://www.crl.mcmaster.ca/People/Faculty/Luo/luo.html>
- [40] M. C. Jeruchim, P. Balaban, and K. S. Shanmugan, *Simulation of Communication Systems*. New York: Plenum, 1992.
- [41] D. Slepian, "Prolate spheroidal wave functions, Fourier analysis, and uncertainty—V: The discrete case," *Bell Syst. Tech. J.*, vol. 57, no. 5, pp. 1371–1430, May–June 1978.
- [42] J. Tuğan and P. P. Vaidyanathan, "Globally optimal two channel FIR orthonormal filter banks adapted to the input signal statistics," in *Proc. IEEE Int. Conf. Acoust., Speech, Signal Process.*, vol. III, Seattle, WA, May 1998, pp. 1353–1356.
- [43] P. Moulin, M. Anitescu, K. O. Kortanek, and F. A. Potra, "The role of linear semi-infinite programming in signal adapted QMF bank design," *IEEE Trans. Signal Processing*, vol. 45, pp. 2160–2174, Sept. 1997.
- [44] M. S. Lobo, L. Vandenberghe, S. Boyd, and H. Lebret, "Applications of second-order cone programming," *Lin. Algebra Appl.*, vol. 284, no. 1–3, pp. 193–228, Nov. 1998.
- [45] T. N. Davidson, Z.-Q. Luo, and K. M. Wong, "Design of robust pulse shaping filters via semidefinite programming," in *Proc. Sixth Can. Workshop Inform. Theory*, Kingston, Ont., Canada, June 1999, pp. 71–74.

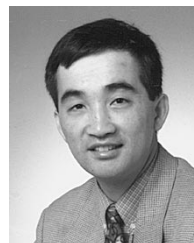


Timothy N. Davidson (M'96) received the B.Eng. (Hons. I) degree in electronic engineering from The University of Western Australia (UWA), Perth, in 1991 and the D.Phil. degree in engineering science from the The University of Oxford, Oxford, U.K., in 1995.

He is currently an Assistant Professor in the Department of Electrical and Computer Engineering, McMaster University, Hamilton, Ont., Canada. His research interests are in signal processing and control, with current activity focused on signal

processing for digital communication systems. He has held research positions at the Communications Research Laboratory at McMaster University, the Adaptive Signal Processing Laboratory at UWA and the Australian Telecommunications Research Institute at Curtin University of Technology, Perth, and brief visiting appointments at QPSX Communications and the Digital Signal Processing Laboratory, The Chinese University of Hong Kong.

Dr. Davidson was awarded the 1991 J. A. Wood Memorial Prize (for "the most outstanding [UWA] graduate" in the pure and applied sciences), and the 1991 Rhodes Scholarship for Western Australia.



Zhi-Quan (Tom) Luo (M'90) was born in Nanchang, China. He received the B.Sc. degree in applied mathematics in 1984 from Peking University, Beijing, China. From 1985 to 1989, he was with the Department of Electrical Engineering and Computer Science, Massachusetts Institute of Technology, Cambridge, where he received the Ph.D. degree in operations research.

From 1984 to 1985, he studied at the Nankai Institute of Mathematics, Tianjin, China. In 1989, he joined the Department of Electrical and Computer Engineering, McMaster University, Hamilton, Ont., Canada, where he is now a Professor. His research interests lie in the union of large-scale optimization, information theory and coding, data communications, and signal processing.

Prof. Luo is a member of SIAM and MPS. He is presently serving as an Associate Editor for *Journal of Optimization Theory and Applications*, *SIAM Journal on Optimization*, *Mathematics of Computation*, and *Optimization and Engineering*.



Kon Max Wong (SM'81) was born in Macau. He received the B.Sc.(Eng.), D.I.C., Ph.D., and D.Sc. (Eng.) degrees, all in electrical engineering, from the University of London, London, U.K., in 1969, 1972, 1974, and 1995, respectively.

He started working at the Transmission Division of Plessey Telecommunications Research Ltd. in 1969. In October 1970, he was on leave from Plessey, pursuing postgraduate studies and research at Imperial College of Science & Technology, London. In 1972, he rejoined Plessey as a Research

Engineer and worked on digital signal processing and signal transmission. In 1976, he joined the Department of Electrical Engineering, Technical University of Nova Scotia, Halifax, N.S., Canada, and in 1981, he joined McMaster University, Hamilton, Ont., Canada, where he has been a Professor since 1985 and served as Chairman of the Department of Electrical and Computer Engineering from 1986 to 1994. He was on leave as a Visiting Professor with the Department of Electronic Engineering, Chinese University of Hong Kong. He is now the Mitel Professor of Signal Processing at McMaster University. His research interest is in the area of signal processing and communication theory.

Prof. Wong received the IEE Overseas Premium in 1989 and is a Fellow of the Institution of Electrical Engineers, the Royal Statistical Society, and the Institute of Physics.